Dynamic emergency route planning for major chemical accidents: models and application

Abstract: Combining scenario construction with the characteristics of individual emergency behavior is necessary for the emergency route planning of major chemical accidents. We investigated this challenging decision problem and constructed a multi-indicator emergency risk assessment method that considers the evacuation speed of different population types and health consequences caused by various risk components. We also designed a modified Dijkstra algorithm to solve this dynamic multi-objective route planning problem. The comparative experiment results demonstrated that the proposed algorithm performs relatively better than the traditional Dijkstra algorithm. Finally, we performed extensive case studies where our simulation results demonstrate that the proposed model provides reliable and practical emergency route planning services for various personnel types under different accident scenarios. Compared with the commonly used single-dimensional assessment method, this comprehensive and informative assessment of the emergency risks faced by the population in different regions could serve as a useful reference for the formulation and implementation of emergency plans in case of major chemical accidents.

Keywords: emergency route planning; dynamic optimization; the modified Dijkstra algorithm; major chemical accidents; emergency risk assessment.

1. Introduction

The rapid development of the global economy has resulted in the considerable increase in the number of industrial parks or projects involving flammable, explosive, toxic, and hazardous substances in recent years (Zhou and Liu, 2012; Hosseinnia et al., 2018; Reniers and Soudan, 2010). Any anticipated hazards are mainly due to human errors, faulty equipment, poor production management, or inappropriate environmental conditions. These major hazards within a region may lead to accidents such as leaks, fire, explosion, or toxic proliferation (Zhou and Liu, 2012). Two main public protective actions are implemented in such situations: to shelter in place or to conduct emergency evacuations. The first option is preferred if the available shelters can provide adequate protection to the affected population, (Sorensen et al., 2004; Jann, 1989; Ujihara, 1989). However, the number of shelters in any affected area is usually limited and the facilities are often not equipped to provide adequate protection. Hence, the public is commonly protected through evacuation. In either situation, people will always

need to transfer from the affected areas to the designated safety areas, which need to be strategically identified. From a practical perspective, studying emergency route planning is of great significance and value, especially when the population in areas affected by major chemical accidents urgently need to be protected.

Moreover, unlike natural disasters such as earthquakes and hurricanes, major chemical accidents might have adverse effects on the health of the population in the affected area due to their exposure to the ensuing extreme phenomena (e.g., fallout, toxic clouds, thermal radiation, overpressure, or fragments) (Georgiadou et al., 2007). Accurate measurement of these adverse effects is the key to choose the correct emergency response plan. Several studies in these areas, including many interesting simulation models, have been produced. Many of these studies describe the temporal and spatial distribution of the toxic gas diffusion concentration after the leakage of hazardous chemicals (Kim, H et al., 2019; Jeong and Baik, 2018) or calculate the occurrence of hazardous factors such as shock wave generated by fire and explosion in hazardous chemical accidents (Ding, et al., 2020; Khakzad, 2018).

Emergency route planning can be regarded as a shortest-path problem where the aim is to find the path with the smallest sum of weights of the constituent edges between two nodes in the graph (composed of nodes and paths) (Shimbel, 1953; Yadav and Biswas, 2010). To solve the problem of route selection in emergency response, among the existing studies on emergency evacuation management, several models and algorithms based on network theory, especially under disaster conditions, are available (Yi and ÖZdamar, 2007; Shi et al., 2012; Georgiadou et al., 2010; Xiao et al., 2001; Yuan and Wang, 2009; Stepanov and Smith, 2009; Zhang et al., 2013; Georgiadou et al., 2007). Various objective functions are used to evaluate the quality of the solutions (Vermuyten et al., 2016). Most of them take time as an optimization objective, and only a few consider the health threats of major chemicals to evacuees. Yoo and Choi (2019) proposed an evacuation plan that needs to be selective enough to consider the indoor and outdoor concentrations of nearby buildings and the time in which the maximum allowable concentration may occur. Zhang et al. (2017) built a mixed-integer programing model that aims to minimize the concentration of hazardous chemicals where people are exposed during the entire evacuation process. When an individual wears no protective equipment and if the chosen emergency route considers minimizing transfer time only, the individual may suffer from serious health consequences during the emergency transfer. Another point that is worth stressing is that the obtained optimal route transit time may be far from satisfactory if only mitigating health consequences are considered. Moreover, the effect of protective equipment, including respiratory equipment, can significantly vary due to the time limit used.

Given the integration and linkage between the activities of companies within the industrial area, these activities are usually close to each other (Hosseinnia et al., 2018). If a

major chemical accident occurs in such chemical clusters, then a domino effect occurs (Cozzani et al., 2005; Jia et al., 2017; Ding, et al., 2020; Khakzad, 2018). Under such circumstances, new challenges and requirements have been added to emergency route planning. For example, on April 16, 2004, a liquid chlorine storage tank exploded in Tianyuan Chemical Plant, Chongqing, China. Two emergency evacuation decisions were made immediately: The first was to evacuate all personnel within the warning area of a radius of 150 m from the accident point, and the second was carried out 4.5 hours after the first order was issued. The plan was to evacuate other personnel within a 1km radius from the accident point because the site headquarters was concerned about potential secondary disasters (around 13 tons of liquid chlorine may explode and leak) (Deng and Jiang, 2009). In the above example, the second evacuation plan showed that when selecting the emergency route, decision-makers must not only consider mitigating the health consequences of the population but also ensure that the affected personnel evacuate safely before secondary disasters could occur.

Many practical factors should be taken into consideration in emergency route selection. An increasing number of researchers have recently been analyzing the impact of the expansion of accidents on the speed of evacuation (Zhang et al., 2013). Yuan and Wang (2009) built a model to describe the effect of disaster extension on the evacuation speed. Some researchers also analyzed the decision-making process of the evacuation. For instance, Smith et al. (2017) apply a cognitive modelling approach for decision making, and use the decision trees to assess the route selection strategy based on training curriculum and simulation for learning. Meanwhile, they further assessed the impact of the environmental and cognitive factorssuch as alarms, fire / smoke, intention, and focus of attention. Recently, Danial et al., (2019) also exploredthe role of human involvement and imagination in decision-making process of evacuation.. In addition, it was found that those evacuees who have social relationships tend to form a group (Hu et al., 2014). Some scholars have modeled the collective phenomena (such as competitive, queuing and herding behaviors) evacuation caused by behavioral characteristics of individuals in crowds (Sharma, 2009). Ling et al. (2018) use the hypothesis of herd behaviour to model the passenger decision-making process.

However, the impact of individual characteristics, emergency warnings, and emergency facilities were not incorporated in their selection strategies. The precursors of major accidents are usually often insufficient, and most warnings are released sometimes after the triggering events (including leaks, fire, explosion, etc.) (Gai and Deng, 2019). Different communication warning channels may cause differences in the time people can access the warning, as highlighted by Gai and Deng (2019). Moreover, during any emergency transfer, the differences in some factors cause emergency risk types (health risks, time risks) and levels to vary significantly, including the speed of different individuals (for example, elderly, youngsters, strong young adults, adults who bring their family with them), protection conditions, and

available safety destination. Thus, their needs for emergency route planning services vary as well (Geogiadou et al., 2010; Carson, 2010; Huang and Chen, 1999). Therefore, providing useful targeted emergency guidance for the population in the affected areas can be rather difficult, if not impossible, if these practical factors are not considered as part of the decision model.

With regard to the risk assessment of evacuation operations, Norazahar et al. (2015) qualitatively discussed the event tree analysis of hazards and consequences. Many scholars have conducted quantitative research based on the data of accident, environmental conditions, human behavior, and organization (Musharraf et al., 2016; Norafneeza et al., 2018; Norazahar et al., 2014). From the perspective of the public, evacuees will inevitably be exposed to risks from accidents or secondary disasters from the departure place to the destination; this situation is also closely related to the chosen evacuation route. Assessing the risks of evacuees during evacuation operations will help in developing a more scientific emergency response plan for people in the area.

In summary, factors such as the expansion of accidents, individual characteristics, emergency warnings, and emergency facilities need to be considered in the model. Decision-makers need to choose their optimization goal(s), which can include time cost and health consequences, depending on the disaster scenario. The proposed model is applied to assess the emergency reaction risk for major chemical accidents. This study attempts to address some of these mentioned aspects.

The contributions of this study are fivefold:

(i) The emergency route planning of multi-disaster scenario due to major chemical accidents is studied. We do not only consider the health consequences caused by the initial incident to the people in the affected area, but also we take into account the time pressure of the evacuation caused by the possible secondary disasters.

(ii) A multi-indicator emergency risk assessment method based on health risk and time risk is proposed. It can provide a more comprehensive and informative risk assessment than the commonly used single-dimensional assessment method.

(iii) A modified Dijkstra algorithm is designed to solve the dynamic multi-objective route planning problem. It overcomes the weakness of the traditional Dijkstra algorithm, which results in a local optimum. The feasibility of the proposed algorithm is proven by comparing its results with those of the traditional algorithm.

(iv) An extensive sensitivity analysis based on a case study is also performed. It mainly studies the impact of departure time and evacuees speed on the optimal route and contributes to the identification of risk areas and key populations.

(v) A strategic plan for major accidents that can be adopted in practice is presented. Considering the disaster scenarios, individual protective conditions, the time of

concerning warnings, the degree of speed, democratic composition, and other practical factors, the proposed plan provides a reference for a public protection plan during major chemical accidents.

The rest of this paper is organized as follows: Section 2 introduces the formulation of the problem and its modeling. Section 3 presents the solution method. Section 4 illustrates the proposed algorithm through a case study from an emergency evacuation network. Section 5 summarizes the conclusions and highlights some research avenues.

2. Modeling of Dynamic Emergency Route Planning for Major Chemical Accidents

2.1 Formulation of emergency network

To facilitate the analysis of emergency route planning in major chemical accidents, we divide the emergency response area into several sub-areas. From the source node where a given affected population is, say v_s, the emergency route destination node, say v_d, can be determined according to the selected protective actions. We consider the entrance of the emergency response area as the node v_d. In the case where a shelter in place is conducted, the nearest shelter building will also be considered v_d. instead. The connection ability between nodes v_i and v_j is denoted by the arc (v_i, v_j).

We define our emergency network by a directed graph $G(V, A)$, where $V = V_s \cup V_d$, with $V_s = \{v_s | \ s = 1, 2, \cdots, n_s\}$ and $V_d = \{v_d | \ d = 1, 2, \cdots, n_d\}$ are the set of source nodes (population locations) and the set of destination nodes (entrances of response areas or shelters) respectively; $A = \{ (v_i, v_j) | \ v_i, v_j \in V \}$ is the set of arcs.

Let (x_i, y_i) denote the coordinates of node v_i in the emergency network, and $c_{ij}(x, y, t)$ is the intensity of the adverse effect (e.g., overpressure, concentration of toxic materials, and heat radiation) on arc (v_i, v_j) at point (x, y) and at time t with $(x, y) \in (v_i, v_j)$;

(1) (x,y): the coordinates of a point on the arc (v_i, v_j).

(2) d_{ij}: the expected dose when traveling along arc (v_i, v_j), which is calculated in (Xiao et al., 2001) as follows (Georgiadou et al., 2010; Zhou and Liu, 2012):

$$d_{ij} = \int_{t_i}^{t_j} f\left\{c\left(x, y, t\right)\right\} dt \tag{1}$$

where t_i and t_j denote the time when individuals reach node v_i and node v_j along the arc (v_i,v_j), respectively.

(3) N_p : the number of population types (for example, three types: old, young, parents with families).

(4) $s_{ij,p}(t)$: the travel speed of the population of type p (p = 1, 2, …, N_p) on each arc (v_i, v_j) of the network under disaster conditions at time t.

(5) s_{ij}^{n}: the travel speed of unaffected healthy young adults on arc (v_i, v_j) under normal conditions.

(6) t_s^{w}: the time when the warning was received.

Under normal conditions, the travel speed of individuals may be affected by their own conditions. For example, the travel speed of elderly, children, and disabled people can be significantly lower than that of healthy young adults (Menz et al., 2004). Even the travel speed of healthy young adults may be affected when they help their family members, such as by supporting the elderly and holding young children.

Thus, suppose the time when the event occurs is time 0 and define $s_{ij,p}^{n}$ as the travel speed of population type p (p = 1, 2, …, N_p) on arc (v_i, v_j) under normal conditions. This can be estimated according to the following formula:

$$s_{ij,p}^{n} = \xi \cdot s_{ij}^{n} \tag{2}$$

in which ξ is the influencing coefficient on speed, indicating the extent to which travel speed is affected due to limited mobility or assisting others. The travel speed on each arc of the network under disaster conditions $s_{ij,p}(t)$ may also decrease with the change in time and space, which is described as follows (Georgiadou et al., 2010; Yuan and Wang, 2009; Zhang et al., 2013):

$$s_{ij,p}(t) = s_{ij,p}^{n} \cdot \alpha_{ij} \cdot e^{-\beta_{ij} t} \tag{3}$$

where α_{ij} and β_{ij} are the parameters that determine the decrease in the travel speed function $s_{ij,p}(t)$. $\alpha_{ij} \in (0,1]$ and $\beta_{ij} \in [0,+\infty)$.

2.2 Objective functions considering the impact of secondary disasters

In this section, we discuss three models, which we name models I, II, and III. The first two are similar single objective-type problems and differ only in terms of the objective function used, whereas the latter treats the problem as a bi-objective problem where the objective of the second model is introduced as a constraint.

Model I

If no danger of the possible secondary disasters exists, then the principle for choosing an emergency route is to prioritize safety; the objective is then to mitigate health consequences during the emergency action. After major chemical accidents occur, less exposure of an individual during the transfer corresponds to low health consequences for them (Georgiadou et al., 2007).

Let $W=\left\{\left(v_s,v_{R_1},...,v_{R_K},v_d\right)\mid v_s\in V_s;\ v_d\in V_d;\ v_{R_k}\in V-\{v_s\}-\{v_d\};1\le R_k\le n\ \forall k=2,...,K\right\}$ be the route with K intermediate nodes, which can include both source and destination nodes.

The following additional notation is used.

(1) t_{ij}: the time required to travel through arc (v_i, v_j).

(2) l_{ij}: the length of arc (v_i, v_j).

(3) d_i :the dose at node v_i.

(4) χ_{ij} is the decision variable with χ_{ij} = 1 if arc (v_i, v_j) is included in the fixed route and 0 otherwise.

The formulation of the dynamic emergency route selection (DERS) (model I) for major chemical accidents is described in (4) to (14) as follows:

$$\min\ f_1 = Minimize\left\{\sum_{i=s}^{d}\sum_{j=s}^{d}\chi_{ij}d_{ij}\right\} \tag{4}$$

subject to

$$\int_{t_i}^{t_j} s_{ij,p}(t)dt = l_{ij} \qquad \forall i,\ j=1,2,...,n;\ p=1,...,N_p \tag{5}$$

$$l_{ij}=\sqrt{\left(x_j-x_i\right)^2+\left(y_j-y_i\right)^2} \qquad \forall i,\ j=1,2,...,n \tag{6}$$

$$t_{ij}=t_j-t_i \qquad \forall i,\ j=1,2,...,n \tag{7}$$

$$t_s=t_s^w \tag{8}$$

$$s_{ij,p}\left(t\right)=s_{ij,p}^{\mathrm{n}}\cdot\alpha_{ij}\cdot e^{-\beta_{ij}t} \qquad \forall i,\ j=1,2,...,n;\ p=1,...,N_p \tag{9}$$

$$d_{ij}=\int_{t_i}^{t_j} f\left\{c\left(x,y,t\right)\right\}dt \quad \forall i,\ j=1,2,...,n \tag{10}$$

$$d_s = \int_0^{t_s} f\{c(x,y,t)\}dt \tag{11}$$

$$\sum_{\substack{j=s \\ j\neq i}}^{d} \chi_{ij} - \sum_{\substack{j=s \\ j\neq i}}^{d} \chi_{ij} = \begin{cases} 1 & i = s \\ -1 & i = d \\ 0 & \text{otherwise} \end{cases} \tag{12}$$

$$\sum_{\substack{j=s \\ j\neq i}}^{d} \chi_{ij} \begin{cases} \leq 1 & i \neq d \\ = 0 & i = d \end{cases} \tag{13}$$

$$\chi_{ij} \in \{0,1\} \qquad \forall i, j = 1,2,...,n \text{ and } t_i \geq 0 \, \forall i = 1,...,n \tag{14}$$

where (4) represents the objective of the model, which minimizes the expected dose along a route. Eqs. (5), (6), (7), and (8) are the recursion formulas of the total travel time along a route, which indicate that arc (v_i, v_j) is traveled through with the speed $s_{ij,p}(t)$ during time period t_{ij}. Eq. (9) is the decrease function of the travel speed on arc (v_i, v_j) with the expansion of disasters and the population type. Eqs. (10) and (11) are used to calculate the expected dose on arc (v_i, v_j) along a route. Constraint (12) guarantees a feasible route from the source node v_s to the destination node v_d by restricting the value of χ_{ij}. Considering the feasibility of the evacuation plan and the urgency of emergency response time, a route with loops is not allowed. Therefore, constraint (13) ensures that the routes have no loops. Constraint (14) refers to the binary decision variables and the continuous nonnegative variables. This model has 10 constraints, n^2 binary variables, and n continuous nonnegative variables.

Model II

If an individual wears protective equipment, considering that the effective protection time of this protective equipment is affected by the type of equipment, then the individual needs to reach the safety areas as soon as possible within the effective protection time. Therefore, the formulation of DERS (model II) for major chemical accidents without secondary disaster risk is similar to model I except the objective function given in (15) is used instead. The model is described as follows:

$$\min f_2 = Minimize\left\{\sum_{i=d}^{d}\sum_{j=d}^{d} \chi_{ij} t_{ij}\right\} \tag{15}$$

subject to Eqs. (5)–(14)

In other words, model II varies from model I in terms of the objective function where the

evacuation time t_{ij} is used instead of the dose d_{ij} between nodes v_i and v_j.

Model III

In this model, both objectives are considered simultaneously, with the objective of model I remaining as the main objective function while the objective of the second model is added as a constraint to the model. The latter is used to define the target that needs to be fulfilled based on the availability of the emergency response. The constraints used in the two earlier models remain unchanged. For example, after the initial event occurs, if any risk of secondary disasters is present apart from considering health consequences in the process of emergency route planning, then the impact of the occurrence and development of secondary disasters on the emergency reaction time should also be noted. This problem falls into the scope of multi-objective optimization where the formulation of DERS (model Ⅲ) for major chemical accidents with secondary disaster risks is described as follows:

$$\min f_1 = Minimize\left\{\sum_{i=s}^{d}\sum_{j=s}^{d}\chi_{ij}d_{ij}\right\} \tag{16}$$

$$f_2 = \sum_{i=s}^{d}\sum_{j=s}^{d}\chi_{ij}t_{ij} \le L_{\mathrm{t}} \tag{17}$$

subject to Eqs. (5)–(14)

where L_{t} is the available emergency response time determined by the occurrence and development of secondary disasters.

2.3 Application in emergency response risk assessment

Risk can be broadly defined as a situation in which people or property may suffer adverse consequences (Yoo and Choi, 2019). Hazardous chemical accidents are complicated because major chemical accidents might have adverse effects on the health of the population in the affected area due to their exposure to the ensuing extreme phenomena (e.g., fallout, toxic clouds, thermal radiation, overpressure, fragments). In this paper, the risk associated with the above health sequence is defined as health risk, which can be estimated through the probit function as follows(OGP, 2010; Georgiadou et al., 2010):

$$Y = A + B\ln d \tag{18}$$

where Y is the probit variable. Lethality can be determined according to Y, and A and B are constants.

Individuals may also face potential risks caused by time delay. For example, the public

must transfer from the affected area to the safe place within a certain period of time because of possible secondary disasters and the limited effective protection time of the emergency protective devices they are wearing. In this paper, time risk refers to the combination of other adverse consequences caused by time delay.

In accordance with the emergency route planning results, the emergency response risk of the major accidents can be assessed from both transfer time and health consequences

$$RE_{\mathrm{h}}\left(v_s, P, t_s^{\mathrm{w}}\right)=\sum_{p\in P}\sigma_{s,p}\cdot\left[A+B\cdot f_1\left(W^*\right)\right] \tag{19}$$

$$RE_{\mathrm{t}}\left(v_s, P, t_s^{\mathrm{w}}\right)=\sum_{p\in P}\sigma_{s,p}\cdot f_2\left(W^*\right) \tag{20}$$

where $P = \{p \mid p = 1, 2, \ldots, N_{\mathrm{p}}\}$ is the set of population type at the source node v_s. $RE_{\mathrm{h}}\left(v_s, P, t_s^{w}\right)$ and $RE_{\mathrm{t}}\left(v_s, P, t_s^{w}\right)$ denote the average health consequences and time risk of all population type P at the source node v_s with the receiving warning time t_s^{w} under major accidents. W^* indicates the optimal emergency route found by model I, II, or III. $\sigma_{s,p}$ represents the affected proportion of the population of type p in the total population at node v_s.

Let L_{T} and L_{HC} be the threshold values of the high-risk and low-risk area, respectively. These values can be found using health consequences and time risks. In this study, the emergency risk of the population located at v_s is divided into four levels according to Fig. 1.

a) If $v_s \in$ Area I, then the time risk and health risk are higher than the acceptable level during the emergency transfer of the population located at v_s;
b) If $v_s \in$ Area II, then the time risk of the population located at v_s during the emergency transfer is still within the acceptable level, but the health risks exceed the acceptable level;
c) If $v_s \in$ Area III, then the health risk of the population located at v_s during the emergency transfer is still within the acceptable level, but the time risk exceeds the acceptable level;
d) If $v_s \in$ Area IV, then both the time and health risks of the population located at v_s during the emergency transfer are within the acceptable level.

The above division of the areas can serve as a basis when allocating emergency rescue personnel, evacuation vehicles, protective equipment, and other resources.

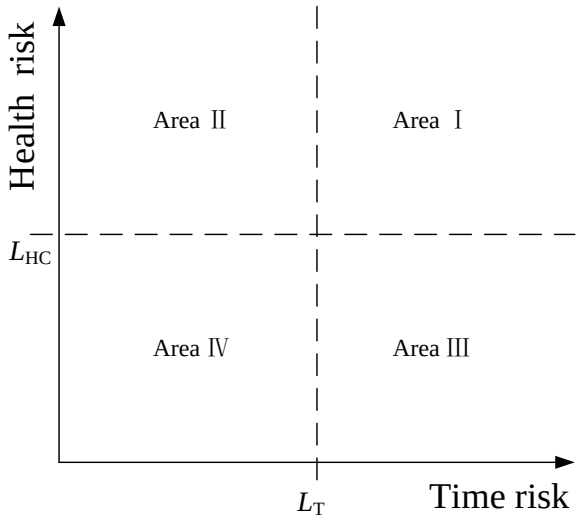

Fig. 1. Multi-indicator emergency risk assessment method for major chemical accidents

3. Algorithm for Emergency Route Planning

Models I and II are both dynamic single-objective models, which can be obtained through the modified Dijkstra algorithm (Yuan and Wang, 2009). In this section, we propose a dynamic bi-objective model inspired by model III, provide its necessary mathematical validity and then present the proposed algorithm. A simple but effective transformation that avoids the algorithm from cycling due to the bidirection of the arcs is also introduced, followed by the correctness of the entire algorithm.

3.1 Model IV

First, we normalize the two objective functions and then use the linear weighted sum method (Mardle and Miettinen, 2000) to convert model III of DERS into a single-objective model as follows:

$$\min F = r_1 \frac{f_1}{f_1^*} + r_2 \frac{f_2}{f_2^*} \tag{21}$$

subject to Eqs. (5)–(14) and (17)
where

$\vec{f} = (f_1^*, f_2^*)^T$ is the ideal point, which is the solution value of the objective functions of Models I and II.

r_1, r_2 refer to the weight coefficients associated with functions f_1 and f_2, respectively, with

$r_1 \geq 0; r_2 \geq 0; r_1 + r_2 = 1$

In the following two lemmas, we will show that the modified Dijkstra algorithm of Yuan and Wang (2009) cannot be used to solve model IV. This limitation led us to develop a modified algorithm accordingly.

Lemma 3.1 Suppose that $s_{ij,p}(t)$ is a monotonically decreasing and integrable function with respect to t when $t \in [0,+\infty)$. Then, t_j is a monotonically increasing function of t_i (Yuan and Wang, 2009).

Lemma 3.2 F_j is not a monotonically increasing function of F_i in the equation $F_{ij} = F_j - F_i$ if $F_i = r_1 \frac{d_i}{f_1^*} + r_2 \frac{t_i}{f_2^*}$.

Proof. Let F_i^k, d_i^k, and t_i^k denote the values of the objective function F given in Eq. (21), the expected dose, and the time when individuals reach node v_i along the route, k respectively, k = 1,2…. And $d_{ij}^k = d_i^k - d_j^k$; $t_{ij}^k = t_i^k - t_j^k$.

Suppose that

$$\begin{cases} F_i^1 = r_1 \frac{d_i^1}{f_1^*} + r_2 \frac{t_i^1}{f_2^*} \\ F_i^2 = r_1 \frac{d_i^2}{f_1^*} + r_2 \frac{t_i^2}{f_2^*} \end{cases} \quad i = 1,2,...,n \tag{22}$$

Here,

$$\begin{cases} F_i^1 - F_i^2 > 0 \\ d_i^1 - d_i^2 < 0 \\ t_i^1 - t_i^2 > 0 \\ f_1^* = c \\ f_2^* = c \end{cases} \tag{23}$$

From node v_i to node v_j,

$$\begin{cases} F_j^1 = r_1 \frac{d_j^1}{f_1^*} + r_2 \frac{t_j^1}{f_2^*} = \frac{r_1}{f_1^*}(d_i^1 + d_{ij}^1) + \frac{r_2}{f_2^*}(t_i^1 + t_{ij}^1) \\ F_j^2 = r_1 \frac{d_j^2}{f_1^*} + r_2 \frac{t_j^2}{f_2^*} = \frac{r_1}{f_1^*}(d_i^2 + d_{ij}^2) + \frac{r_2}{f_2^*}(t_i^2 + t_{ij}^2) \end{cases} \quad j = 1,2,...,n \tag{24}$$

According to Lemma 3.1, $s_{ij,p}(t)$ is a monotonically decable function with respect to t when $t \in [0,+\infty)$, so $t_{ij}^2 > t_{ij}^1$. Here suppose that the function $f\{c(x, y, t)\}$ is a constant and thus $d_{ij}^1 > d_{ij}^2$. Then,

$$F_j^1 - F_j^2 = \frac{r_1}{f_1^*}(d_i^1 + d_{ij}^1) + \frac{r_2}{f_2^*}(t_i^1 + t_{ij}^1) - \frac{r_1}{f_1^*}(d_i^2 + d_{ij}^2) - \frac{r_2}{f_2^*}(t_i^2 + t_{ij}^2)$$
$$= F_i^1 - F_i^2 + \frac{r_1}{f_1^*}(d_{ij}^1 - d_{ij}^2) + \frac{r_2}{f_2^*}(t_{ij}^1 - t_{ij}^2) \quad (25)$$

Obviously, the result of Eq. (25) can be less than 0. Similarly, the result of Eq. (25) can also be less than 0 if $f\{c(x, y, t)\}$ is not a constant.

3.2 The proposed method

For the single-objective route selection model under the real-time effect of disaster extension, Yuan and Wang (2009) proposed a variant of the Dijkstra algorithm to solve the model. This variant is based on the current node's objective function value, which is a monotonically increasing function of its upstream node's objective function value (see Lemma 3.1). According to Lemma 3.2, model IV cannot be solved using this algorithm. To overcome this limitation, we introduced some basic modifications, thus creating a new variant of the well-known Dijkstra algorithm to optimally determine the shortest path. This new variant is performed as follows:

Let $W_E = \{ c_{ij}(x, y, t), t_{ij}, d_{ij}, l_{ij}, \alpha_{ij}, \beta_{ij}, s_{ij}^n, t_s^w \}$ be the set of arc weights. Let the label $P(v_j)$ be the value of min F in Eq. (21) from node v_s to node v_j and the labels T_F, T_1, and T_2 denote the sets of the objective function values (F, f_1, and f_2) of the different routes of the nodes, respectively. Let $S = \{v_m | m = 1, 2, \ldots, n\}$ denote the set of nodes whose shortest route has been found. The main steps used by the proposed method to solve model IV is described in Fig. 2.

In Fig. 2 (a), $N_{\max}$ represents the number of iterations. This parameter can be determined according to the distribution of the solutions in the search space. In Eq. (21), the ideal point values of the different nodes are different, but we consider only the known and determined node for the ideal point value: the obtained $W_j, f_1(v_d), f_2(v_d)$ are the corresponding route, and the values of f_1 and f_2 from node v_s to node v_d when $P(v_d)$ is the minimum objective function value F from node v_s to node v_d. For the other nodes, these corresponding values are the ones assigned to the optimal solutions under Eq. (21) with the ideal point values of v_d.

The DERS algorithm shown in Fig. 2 consists of two parts. The main algorithm is shown in Fig. 2(a), with the calling algorithm presented in Fig. 2(b). In Fig. 2, we first determine the two weight coefficients of the above bi-optimization problem. If it is a single objective problem, then the problem is reduced to having $\vec{r} = (r_1, r_2) = (0,1)$ or $(1,0)$, resulting in the corresponding f_1^* and f_2^* being both 1. In this situation, the algorithm shown in Fig. 2(b) can be applied directly. However, if it is a bi-objective problem, then the best route will be

constructed at the end of the algorithm through a search space constructed by a vector of weight coefficients in Fig. 2(a).

The essential idea behind the calling algorithm of Fig. 2(b) is that when the Dijkstra algorithm is implemented, each additional subsequent node will update the weights of the network based on the route that was found.

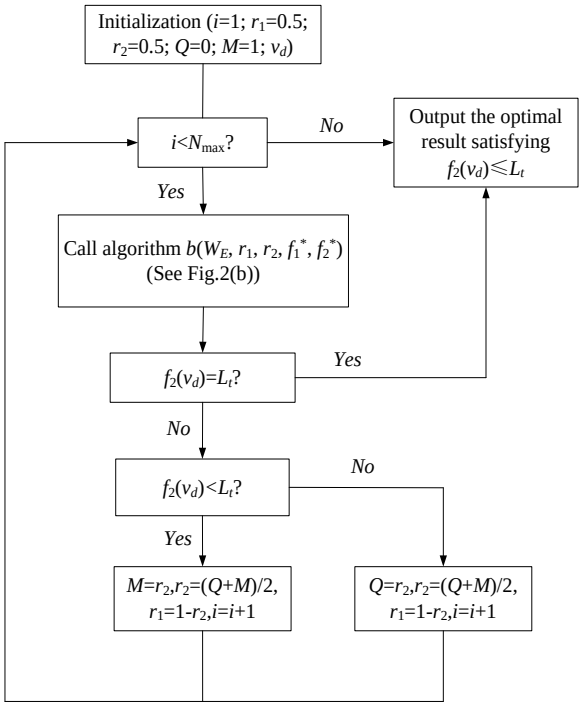

Fig. 2(a). Main algorithm for DERS

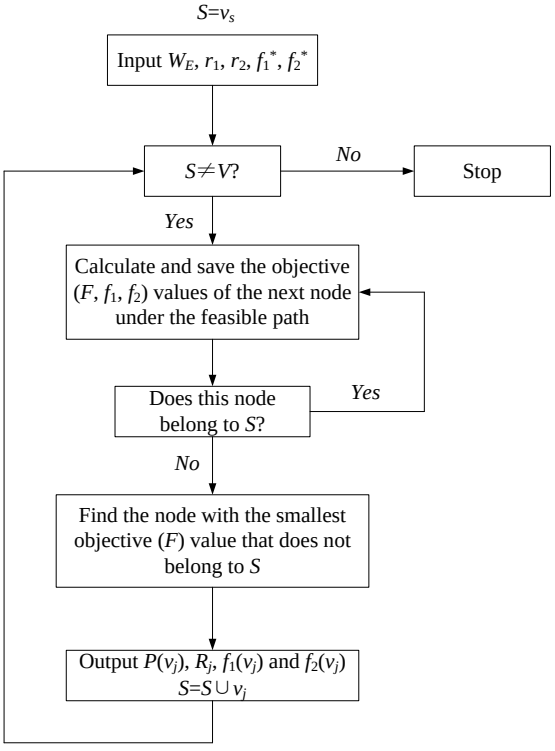

Fig. 2(b). Calling algorithm

3.3 Disposal method in the presence of a bidirectional arc

In the original emergency network, where only safety exits are available. Suppose that there are additional emergency shelters, the nodes within the coverage will increase the number of potential paths that lead to the emergency shelter. This situation will obviously create a two-way system in the network. The problem is that the algorithm may cycle if two-way sides are present, leading to the wrong result. On the basis of the urgency of emergency reaction, we transform the emergency network into two one-way networks to solve this problem. For example, consider Fig. 3, where node 3 is the emergency shelter, with the blue circle representing its coverage, and node 8 is the safety exit of the emergency network. This problem can now be solved according to the location of the transfer population as follows: When calculating the nodes within the coverage of the emergency shelter, we use the network in Fig. 3 (Network *A*); otherwise, we use the network in Fig. 3 (Network *B*).

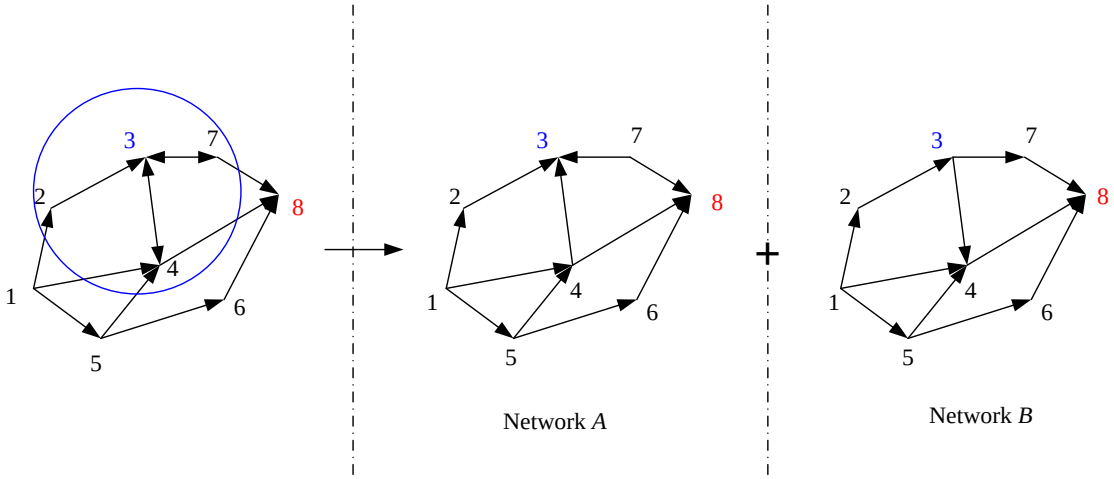

Fig. 3. Schematic of solutions for networks with bidirectional arcs

3.4 Correctness of the proposed algorithm

The following Lemma 3.3 is applied to prove the correctness of the proposed algorithm:

Lemma 3.3. Assume that W^* is the shortest route for model IV, then $f_1(W^*)$ is a monotonically decreasing function of the weight coefficient r_1, while $f_2(W^*)$ is a monotonically increasing function of the weight coefficient r_1.

Proof. Suppose W_1^* and W_2^* are the shortest routes when the weight coefficient r_1 of the objective value f_1 is a and b respectively. Let $a > b \geq 0$, equivalent to $(1-b) > (1-a) \geq 0$, then

$$f_1(W_1^*)\cdot a + f_2(W_1^*)\cdot(1-a) \leq f_1(W_2^*)\cdot a + f_2(W_2^*)\cdot(1-a) \tag{26}$$

and

$$f_1(W_1^*)\cdot b + f_2(W_1^*)\cdot(1-b) \geq f_1(W_2^*)\cdot b + f_2(W_2^*)\cdot(1-b) \tag{27}$$

which leads to

$$[f_1(W_1^*) - f_1(W_2^*)]\cdot a + [f_2(W_1^*) - f_2(W_2^*)]\cdot(1-a) \le 0 \tag{28}$$

and

$$[f_1(W_1^*) - f_1(W_2^*)]\cdot b + [f_2(W_1^*) - f_2(W_2^*)]\cdot(1-b) \ge 0 \tag{29}$$

Therefore, we can deduce that

$$f_1(W_1^*) - f_1(W_2^*) \le 0 \tag{30}$$

and

$$f_2(W_1^*) - f_2(W_2^*) \ge 0 \tag{31}$$

On the basis of the above proof and Lemma 3.3, the range [0,1] of the weight coefficient can be taken as the search space, and a simple dichotomy search can then be used to refine the search interval, leading to the solution of model IV.

On the basis of the above definitions and Lemma 3.2, the correctness of the algorithm in Fig. 2(b) can be proved by recurrence as follows:

(1) When $S = v_s$, the conclusion is obviously true.

(2) Suppose that the conclusion is right when $S = S \cup v_n$, i.e., for each node v_j where $v_j \in S$, and $P(v_j)$ is the minimum objective value F from node v_s to node v_j.

(3) Let us prove whether the algorithm remains valid when $S = S \cup v_{n+1}$. From the algorithm in Fig. 2(b), $F(v_j) = \min_{v_j \notin S} T_F(v_j)$ and $P(v_x) = \min_{v_j \notin S}\{F(v_j)\}$, $S = S \cup v_x$ can be obtained.

Suppose that H is an arbitrary feasible route from node v_s to v_x. Given $v_s \in S$ and $v_x \notin S$, along route H, an arc exists whose origin node is in S while the destination node is not in S. Now, suppose that (v_r, v_l) is the first one among those arcs along route H, i.e., $v_r \in S$, $v_l \notin S$. When $v_l = v_x$, according to Lemma 3.2, the shortest route of v_r is assumed to be found, which means $P(v_r) = F_r^1$. $F_r^H > P(v_r)$, but F_x^H along this route is less than F_x^1 along the shortest route of v_r, In this case, $W_x \neq W_r \cup v_x$. This concept also proves that the modified Dijkstra algorithm proposed by Yuan and Wang (2009) cannot be used to solve the DERS model. When the algorithm selects the next node, it recognizes the shortest route of the upstream node as the only route to calculate the objective value and ignores the correct route to minimize the objective value of the node. With the introduction of the loop of "Does this node belong to S" in Fig. 2(b), $T_F(v_x)$ now contains all the objective values calculated along the route, which means that all nodes in the route belong to the set S. When $v_l \neq v_x$,

$P(v_x) = \min_{v_j \notin S}\{F(v_j)\} \le \min_{v_j \notin S} T_F(v_j) < F_j^H + F_{jx}^H$. This idea is true because of the nonnegative nature of the weighted sum objective value *F*. In other words, $P(v_x)$ is the minimum objective value *F* from node v_s to node v_x.

4. Computational Results

In this section, we first introduce the case that will be used for our computational experiments followed by an illustration of Lemmas 3.2 and 3.3. Some computational results and analysis are then produced for the case of without and with secondary disaster risks.

4.1. Introduction and description

Fig. 4 is an emergency network that has 20 nodes; the coordinates of each node in the network are shown in Table 1. The initial traveling speed s_{ij}^{n} and the speed attenuation parameters α_{ij} and β_{ij} are given in Table 2. Assume that a liquid ammonia tank at node 1 leaks. A set of concrete parameters (leakage parameters, meteorological conditions, etc.) are selected to calculate the consequences of the leak, as shown in Table 3. For the convenience of calculation, the Gaussian plume model is used to calculate the ammonia concentration at each node (Ding et al., 2007). On the basis of the vulnerability of humans (OGP, 2010), the toxicant dose absorbed by an evacuee through a certain arc can be estimated by the following formula:

$$d_{ij} = \int_{t_i}^{t_j} \left(\frac{C_i + C_j}{2}\right)^n \tag{32}$$

where C_i, C_j are the concentration of ammonia at nodes v_i and v_j. ppm; and n is the power exponent, which is $n = 2$ for ammonia.

The probit recommended below is published by a recognized body (Netherlands Organization for Applied Scientific Research) and used by regulators. *A* and *B* in Eq. (21) are −16.33 and 1, respectively. Suppose that the thresholds of high-risk and low-risk areas are determined based on health risk and time risk are $L_{HC} = 2.51$ and $L_T = 8.0$, respectively.

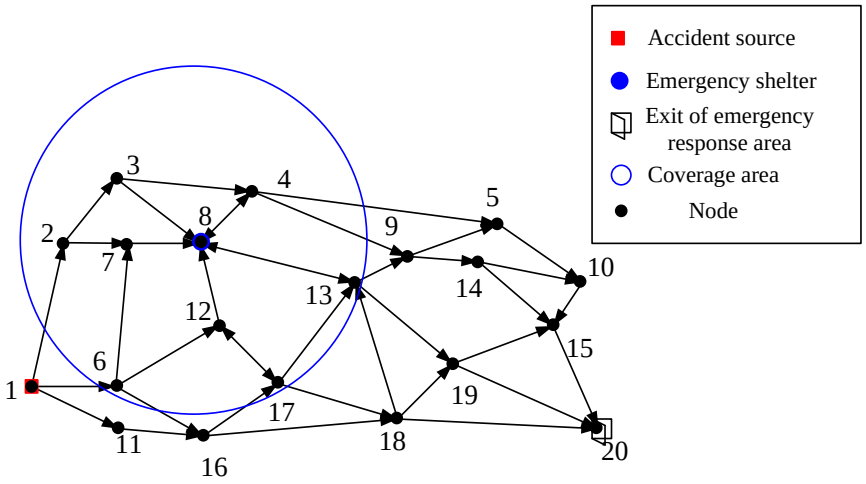

Fig. 4. Emergency network structure

Table 1 Coordinates of nodes

Node	**(*x*, *y*)**	**Node**	**(*x*, *y*)**	**Node**	**(*x*, *y*)**	**Node**	**(*x*, *y*)**
1	(0,0)	6	(130,0)	11	(135,−65)	16	(265, −76.123)
2	(50,221.02)	7	(150,220)	12	(290,94.893)	17	(380.46,4.433)
3	(130,320)	8	(260,220)	13	(500,160)	18	(565,−50)
4	(340,300)	9	(580,200)	14	(690,191.575)	19	(650,35)
5	(720,250)	10	(850,160)	15	(805,92.861)	20	(875,−65)

Table 2 Evacuation network structure and speed parameters

(v_i,v_j)	$(s_{ij}^n,\alpha_{ij},\beta_{ij})$(m/min,-,-)	(v_i,v_j)	$(s_{ij}^n,\alpha_{ij},\beta_{ij})$(m/min,-,-)	(v_i,v_j)	$(s_{ij}^n,\alpha_{ij},\beta_{ij})$(m/min,-,-)
(1,2)	(100,0.85,0.07)	(6,16)	(75,0.86,0.09)	(14,10)	(115,1,0)
(1,6)	(60,0.83,0.07)	(7,8)	(90,0.89,0.08)	(14,15)	(105,1,0)
(1,11)	(115,0.84,0.09)	(8,4)	(85,0.92,0.03)	(15,20)	(30,1,0)
(2,3)	(60,0.88,0.09)	(8,13)	(75,0.92,0.01)	(16,17)	(115,0.85,0.06)
(2,7)	(70,0.82,0.06)	(9,5)	(65,1,0)	(16,18)	(70,0.83,0.05)
(3,4)	(100,0.98,0.01)	(9,14)	(90,1,0)	(17,13)	(80,0.91,0.02)
(3,8)	(95,0.95,0.01)	(10,15)	(35,1,0)	(17,18)	(75,0.95,0.04)
(4,5)	(120,0.99,0.01)	(11,16)	(70,0.89,0.07)	(18,13)	(45,0.99,0.02)
(4,9)	(85,0.98,0.02)	(12,8)	(65,0.99,0.02)	(18,19)	(110,0.97,0.01)
(5,10)	(50,1,0)	(12,17)	(100,0.95,0.03)	(18,20)	(120,0.93,0.04)
(6,7)	(65,0.85,0.05)	(13,9)	(40,0.98,0.05)	(19,15)	(75,1,0)
(6,12)	(105,0.82,0.06)	(13,19)	(120,0.98,0.04)	(19,20)	(100,1,0)

Table 3 Parameter specification

Leakage parameter		Meteorological parameters	
Volume (m^3)	50	Average temperature (℃)	25
Cleft shape	Circular	Average wind speed (m/s)	3.5
Cleft diameter (mm)	100	Prevailing wind direction	East wind
Cleft height (from the ground) (m)	2.4	Solar radiation intensity	Weak
Cleft height (from liquid level) (m)	1.3		
Internal pressure (pa)	1000000		
Density (kg/m^3)	608		
Height measured (m)		1.67	

4.2. Illustration of Lemmas 3.2 and 3.3

In this subsection, an example is analyzed to illustrate the theoretical results discussed in the previous section. To compare with the modified Dijkstra algorithm proposed by Yuan and Wang (2009), we use their data and model to perform our computational experiment. The algorithms were implemented in Java and run on a PC with 2.60 GHZ CPU and 16 GB RAM. Table 4 illustrates the process of solving the shortest route from node v_1 to node v_{20}. The result obtained by the algorithm is different from that achieved by Yuan and Wang (2009), as shown in Table 4.

Table 4 Shortest evacuation route obtained through the method illustrated in Fig. 2(b) and the modified Dijkstra algorithm proposed by Yuan and Wang (2009)

r_1	Route	F	method
0.77	1→6→12→17→18→20 (W^1)	0.084	the algorithm illustrated in Fig. 2 (b)
	1→11→16→18→20 (W^2)	0.085	the modified Dijkstra algorithm proposed by Yuan and Wang (2009)

In summary, W^1 is shorter than W^2 with respect to the optimization objective function shown in Eq. (12) by Yuan and Wang (2009).

In addition, the F value of the route 1→11→16→18 (W^3) is −0.33042842, which is smaller than $F = -0.33042841$ of the route 1→6→12→17→18 (W^4). However, results show that W^4 is part of the shortest route when node 20 is the destination node. This observation is supported by Lemma 3.2 because the objective function is not an increasing function.

In the proposed method, while obtaining the shortest route at node 18, the objective value of the route W^4 is recorded and the target value of the subsequent nodes is updated accordingly. This is not the case for the modified Dijkstra algorithm proposed by Yuan and Wang (2009), which misses the correct shortest route because it does not incorporate backtracking in its

search.

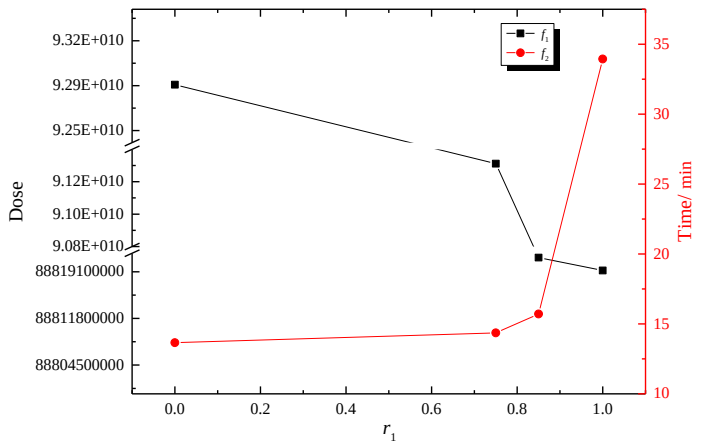

Fig. 5. Dose and time by model IV with respect to r_1

On the basis of the data in Section 4.1, the curves of f_1 and f_2 are shown in Fig. 5 when the weight coefficient r_1 varies from 0 to 1 while the other parameters are kept fixed. The simulation results are consistent with the theoretical analysis of Lemma 3.3.

4.3. Results for major accidents without secondary disaster risks

Here, we analyze the case when no secondary disaster occurs.

Assume that the speed of individuals at the source nodes is affected by the influencing factor $\xi = 1$. People located at the nodes within the coverage of the emergency evacuation shelter take the shelter as their destination, and those at other nodes take the exits of the emergency response area as their destination. Those who are outside the coverage will not venture into the emergency shelter because of the limitation of the evacuation shelter. The assumptions here are that the time for everyone to receive the warning $t_s^{\mathrm{w}} = 0$ and that no risk of secondary disasters exists.

On the basis of Models I and II, the emergency route planning results of each node can be obtained according to whether or not personnel wear protective respiratory devices or not (see Appendix 1). This situation is of great significance to the overall planning of the evacuation network, given that people in the affected area are evacuated from more than one location. The health consequences of personnel taking emergency actions at each node are shown in Fig. 6 for Models I and II.

Figs. 4 and 6 show that if more routes can be chosen between the source node and the corresponding destinations (such as nodes 1, 3, 11, and 16), then the optimal emergency route for the same node obtained based on Models I and II are different. On the whole, the difference in health risks obtained between different nodes with the same objective is relatively too large.

This situation occurs not only because of the location of the node and the wind direction will cause the difference in the concentration of toxic gas diffusion between each other but also because the different evacuation destinations will also affect the health risk of the evacuees. For example, the positions of nodes 13 and 9 in the network are roughly the same, but because the evacuated people of node 13 can go to the emergency shelter, the health risk is much smaller than that of node 9. This finding shows that well-protected emergency shelters have a very significant effect on reducing the impact of accidents and reducing the risk of evacuation. However, reasonable planning of the location and capacity of emergency shelters is critical to ensuring public safety because of the constraints of cost and urban space. Moreover, the health consequences of the optimal route calculated through model II are relatively higher than those calculated through model I. This finding indicates that when the individual does not wear a respiratory protective device and if the transfer time is the only optimization objective function in route planning, then the individual may face much higher health risks during the emergency transfer.

On the basis of health consequences and transfer time, the emergency reaction area is divided into high-risk area and low-risk area. On the basis of model I, the assessment results over the emergency route planning of each node evaluated by Eq. (19) are displayed in Fig. 7(a). The evaluation results of Eq. (20) based on model II are shown in Fig. 7(b). (Nodes 8 and 20 do not perform calculations because they are destination nodes.) We can conclude through Fig. 7(a) that if individuals wear no respiratory protective devices and are located at nodes that are far away from the destinations (including nodes 1, 6, 11, 16, 17, 18, and 19), then their health is at higher risk. The result of Fig. 7(b) shows that nodes 1, 5, 9, 10, 11, and 16 are in the high-risk area.

A comparison between Figs. 7(a) and 7(b) shows that when applying Models I and II, respectively, the division results of the health risk and time risk corresponding to the emergency routes overlap, although some differences still exist. The differences can be significant when the source node is close to the poisonous gas diffusion direction and closer to the destination or the source node deviates from the poisonous gas diffusion direction and farther from the destination, such as nodes 9, 17, 18, 19, and 6. If model I or II is adopted only to find the emergency route of each node, then the assessment results of the time risk and health risk hardly reflect the overall emergency risk level corresponding to each node， At the same time, it may also put evacuees in a dangerous situation. For example, when only time risk is considered, the evacuation route chosen by the evacuees at node 17 is low risk, but it will pose serious health threats, which is unbearable. From the perspective of choosing the optimal emergency route, the area division results will not only affect the overall emergency action but also determine the whole emergency network risk warning system planning and the evacuation plan design. The necessary step is to give people in high-risk areas early warning

notices and allow them to enter well-protected emergency shelters or safe places as soon as possible. In summary, we need to provide a comprehensive reference for the public protection plan of major chemical accidents according to the personnel protection situation and the number of regional refuge facilities.

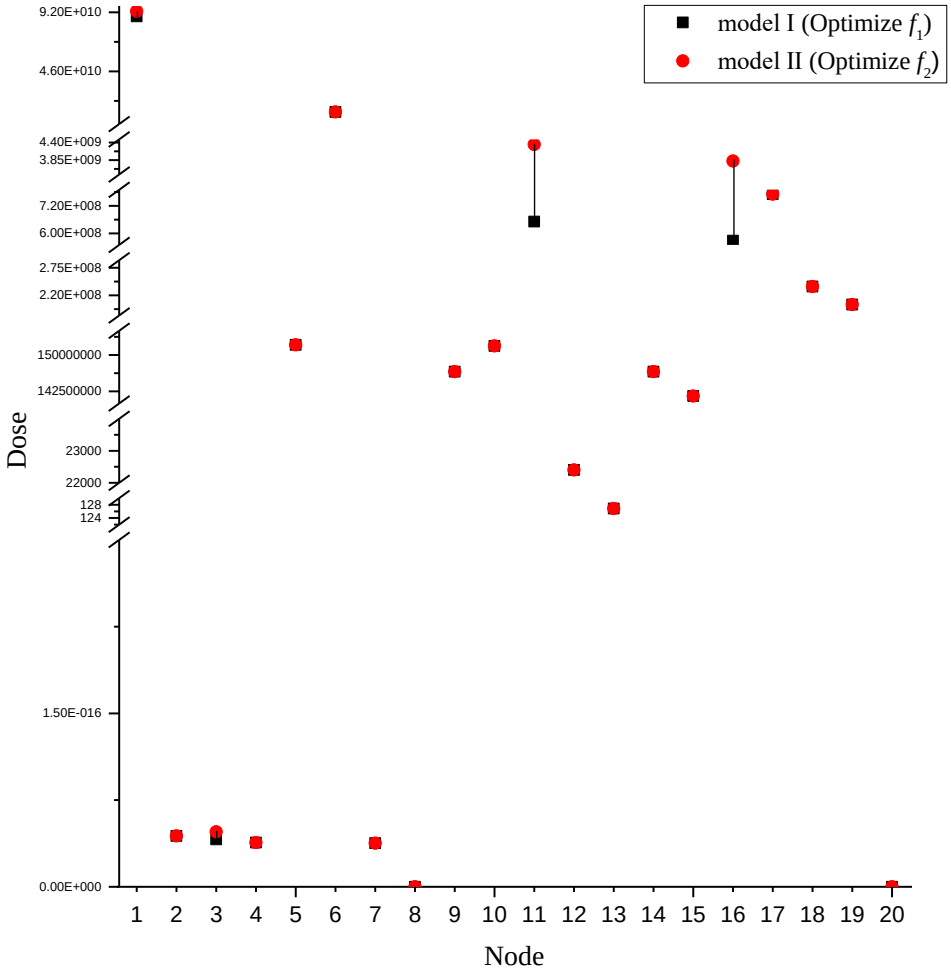

Fig. 6. Dose obtained by emergency route planning based on Models I and II for different source nodes

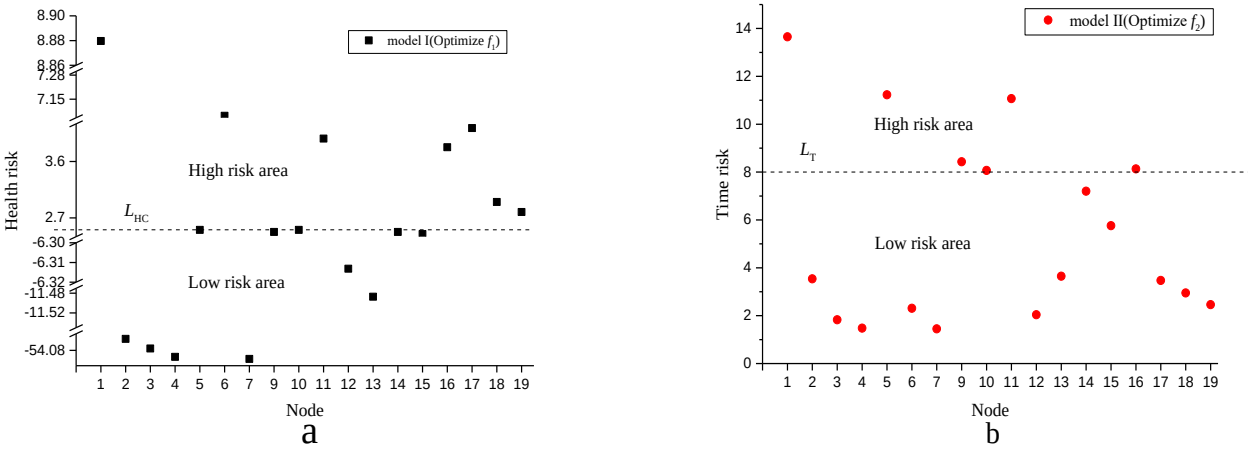

Fig. 7. Risk area division based on Models I and II: (a) optimize f_1 and (b) optimize f_2

We can also test the impact of the warning time and the level of the speed on the effect of the emergency route planning results and risk assessment, as shown in Figs. 8 and 9.

Fig. 8 shows the emergency risk of the optimal routes for node 14 on the basis of Models I and II with respect to t_s^w. From Fig. 8, whether the personnel located at node 14 wear protective devices or not, if the warning time is delayed, then their health and time risks will increase correspondingly during their emergency transfer. If the period between the occurrence of the accident and the time warning reaches 1 minute, then the emergency time risk will increase from a low to high. If this amount reaches 3 minutes, then the emergency health risk will elevate to a high level. Fig. 9 shows the emergency risk of the optimal routes for different population types of node 15 on the basis of Models I and II. As shown in Fig. 9, the extent of speed being affected is increased for the population located at node 15, resulting in increased health and time risks during the emergency transfer. When the speed influencing coefficient ξ decreases to 0.8, the emergency health risk will rise from a low to a high level; when it ξ decreases to 0.6, the emergency time risk will increase from a low to a high level. The evacuation area includes not only healthy adults but also a certain number of children and the elderly. In emergency evacuation operations, if slower-moving people are not assisted in avoiding danger, then the safety of the group will be more threatened compared with that of healthy adults.

Simulation results

The simulation results show that the proposed dynamic emergency route planning model helps identify high-risk groups and assists in optimizing emergency resource allocation on the basis of several factors: disaster scenarios, individual protective conditions, time of releasing warnings, and degree of speed, among others.

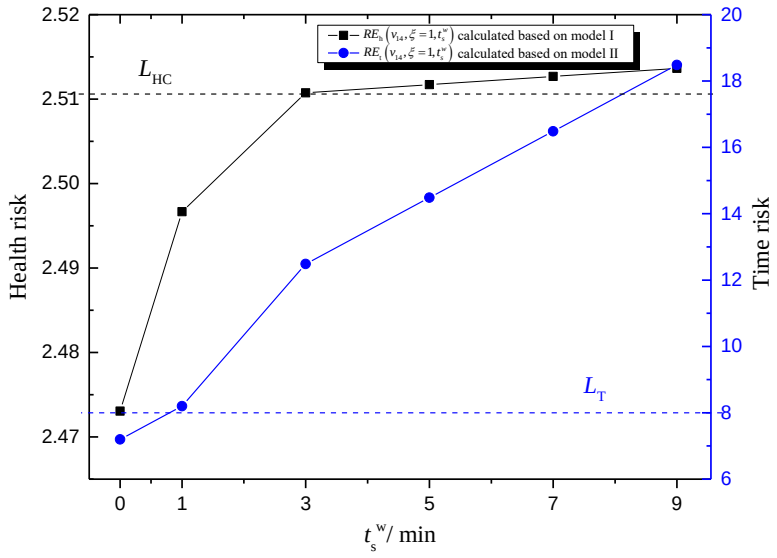

Fig. 8. Emergency risk of the optimal routes for node 14 based on Models I and II with respect to t_s^{w}

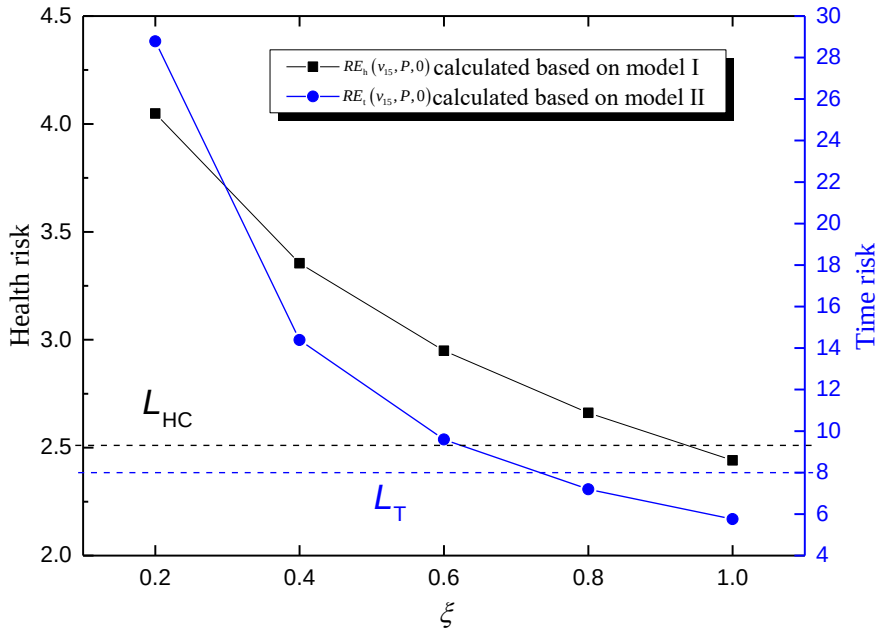

Fig. 9. Emergency risk of the optimal routes for node 15 based on Models I and II with respect to ξ

4.4 Results of dynamic route selection for major accidents with secondary disaster risk

In this case, we examine the case when secondary disaster risks exist.

Assume that the available emergency reaction time L_t = 16 minutes under the threat of secondary disaster, while the speed influencing coefficient of the population at the source node

ξ = 1 and the time the warning is received t_s^w = 0. Also, suppose that the emergency shelter cannot provide adequate protective devices and all personnel in the emergency network need to transfer to safety exits. The proposed algorithm can solve model III and obtain the optimal emergency route for each node and thus help evaluate the emergency risk of different regions (Appendix 2).

Appendices 1 and 2 suggest that the optimal emergency route obtained through model III is sometimes a tradeoff between the solutions that corresponds to the ideal point (such as node 1). If the emergency route found by model I or II in the current accident scenario is still adopted, then the population may face higher time or health risk. Moreover, for the nodes within the coverage area of the emergency shelter, individuals may choose the optimal route either to the emergency shelters that meet the shelter requirements or through the emergency response area exits to destination areas. The latter presents significant higher risks than the former.

On the basis of the results of Appendix 2 and the multi-indicator emergency risk assessment proposed in Section 2.3, the nodes in the emergency network are divided into different emergency risk areas, as shown in Fig. 10. Compared with the emergency risk area division under the single indicator in Fig.7, the emergency risk area division method in Fig. 10 reflects clearly both the level of health and time risks during the emergency transfer of the population at each node. The priority should be protecting the people in this area because of the relatively high health and time risks of the node in Area I. In addition to the necessary emergency early warning system and emergency protective equipment, an emergency shelter that meets protection conditions can be established to reduce casualties; nodes located in Area II have higher health risks and lower time risks. Sufficient emergency protective equipment is more needed by people in this area; nodes located in Area III have higher time risks and low health risks. A scientific and complete emergency early warning system should be established for this area to buy precious time for the evacuation of the people in this area; the two risks of the node located in Area IV are relatively low and can be taken under the premise of considering other conditions such as cost due to necessary emergency management measures. In summary, the results can comprehensively demonstrate the emergency risk level of the people in different areas affected by major chemical accidents. This information provides reference for the formulation and the implementation of major chemical accident emergency plans.

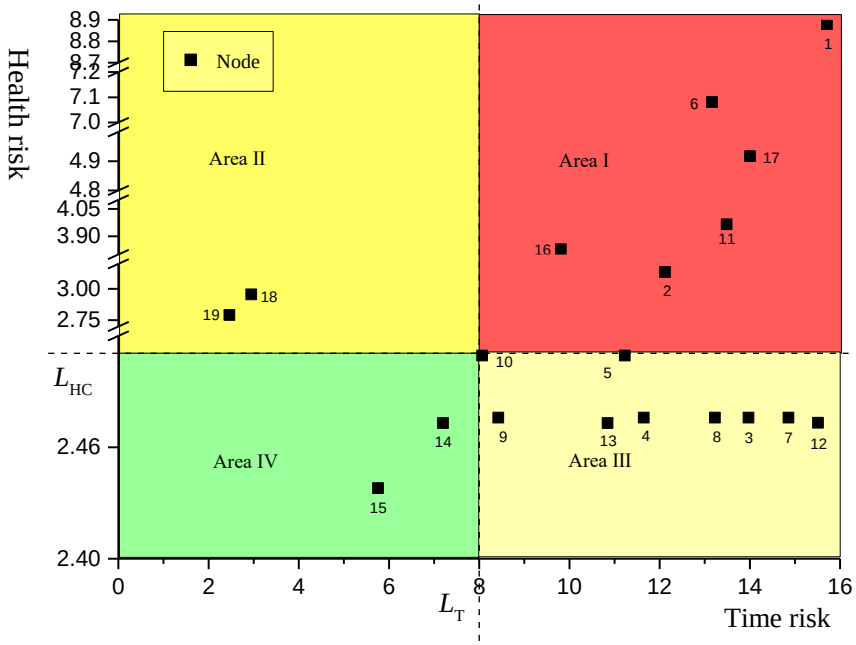

Fig. 10. Area division results of the multi-indicator emergency risk

For example, on the basis of model III, node 14 is selected to help analyze the influence of demographic composition on the emergency risk area division. The population is divided into two groups: $\xi = 0.5$ for people affected and $\xi = 1$ otherwise. On the basis of the multi-indicator emergency risk assessment method proposed in Section 2.3, the change in the risk area division at node 14 with $\sigma_{14,\xi=0.5}$, which is the ratio of those whose speed get affected to the population, is shown in Fig. 11. We can conclude from Fig. 11 that if this ratio goes up, then the whole area's emergency risk level will increase. In addition, if the ratio is greater than 20%, then the emergency risk will reach a high level.

The simulation results show that the dynamic emergency route planning model helps identify high-risk populations considering both health and time risks on the basis of various factors such as disaster scenario and the ratio of people whose speed is affected, among others. In other words, this approach further optimizes the allocation of emergency resources.

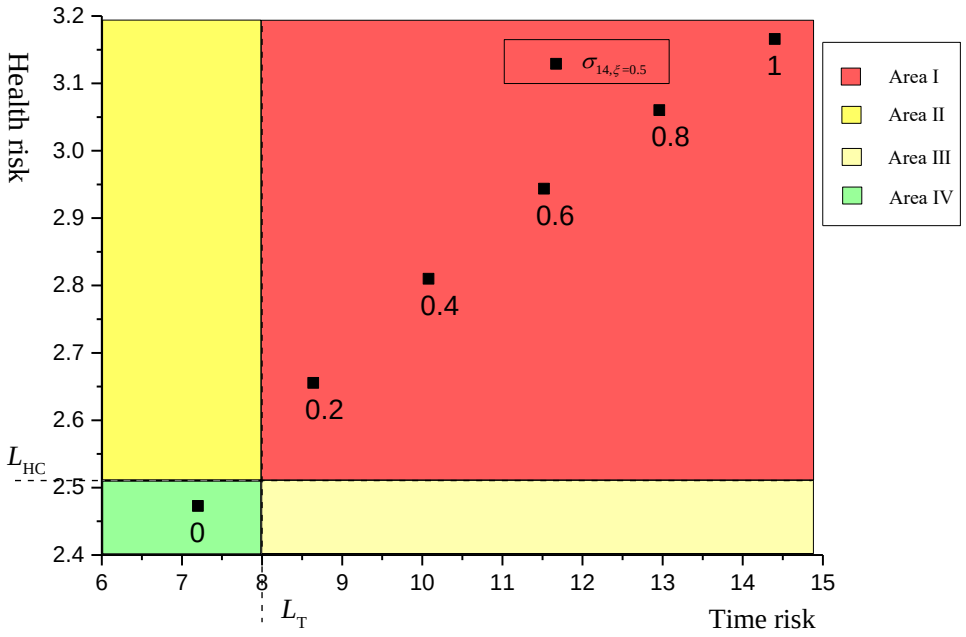

Fig. 11. Corresponding risk of node 14 changes with $\sigma_{14,\xi=0.5}$

5. Conclusions and Future Research

Emergency route planning for major chemical accidents is different from that for natural disasters such as earthquakes and hurricanes. Major chemical accidents are characterized by delay in early warning and possible secondary disasters, which is why considering various factors in emergency route planning is necessary. These factors could include possible secondary disasters (such as fire caused by explosion, explosion caused by leaks, leaks caused by explosion, and others), expansion of accidents, warning release time, the level that individual speed is affected, emergency facilities, and demographic composition, among others. In this study, we propose a dynamic emergency route planning model for major chemical accidents. Our study considers the abovementioned factors and takes one or more factors in health consequences or transfer time as the optimization objective functions. We propose a modification of the well-known Dijkstra algorithm to deal with the bi-objective optimization problem for emergency route selection under the real effect of disaster extension for major chemical accidents. As a byproduct of the study, we also propose an interesting and informative individual emergency risk classification method for major chemical accidents that takes both health consequences and transfer time risk into consideration.

Simulation results show the feasibility and advantages of the models and algorithms presented in this paper. In brief, the following summary outcomes are obtained:

a) First, the optimal route based on different optimization objectives may vary. This is mainly determined by the complexity of the emergency network. At the same time, when an individual does not wear any protective devices, the emergency route planning strategy that chooses the optimization of transfer time as the objective may end up exposing people to higher health risks. For example, the time risk of the evacuation route based on Model II at node 1 is only reduced by (11.07-13.49) / 13.49 × 100% = 17.9%, but the health risk is increased by (5.86114-3.96556) / 3.96556 × 100% = 47.8%.
b) Second, the later the people receive the warning,the longer they will stay in the affected area, and consequently their health and time risks during transfer will also increase accordingly. For those whose speed is affected due to limited mobility or assisting others, their health and time risks are also higher than those of healthy young adults.
c) Third, traveling to a nearer emergency shelter that meets shelter requirements is safer for the population than adding safety exits. This can not only reduce the evacuation time, but also decrease the health threat brought by the accident. This may need to have certain requirements for the protection effect of shelter requirements in the case of no secondary disaster.
d) Fourth, in emergency response area risk assessment, the demographic constituent should be taken as a factor that demands attention. With the increase in the ratio of people in the emergency reaction area whose evacuation speed is affected, the total regional risk will increase accordingly.

In summary, the proposed dynamic emergency route planning model can be used to identify the population that faces high health and time risks according to disaster scenarios, individual protective conditions, warning release time, the affected extent of speed, and the proportion of people whose speed is affected to the total population, among other factors. This scheme can provide a reference for the optimization of emergency resource allocation and the formulation and the implementation of effective emergency plans.

This study can be extended as follows:

(i) The proposed optimization algorithm can be applied to similarly constrained optimization problems, such as route selection of emergency rescue teams caused by other disasters, logistics management, and other fields. In addition, the results of the optimal path of different nodes in the network can provide references for the allocation of shelters and emergency resource management in emergency management.
(ii) This paper mainly studies the evacuation behavior of individuals in emergency response. The main factors that were used are individual characteristics and departure time. These details can be combined with the development of smartphone technology, which allows specific emergency evacuation guidance to be

systematically provided for specific individuals when a disaster occurs. Future research can also cover the limitations of group factors in emergency actions, such as the impact of people flow on individual speed.

(iii) The regional emergency risk assessment results are combined with the new generation of information technology, such as big data and spatial geographic information integration. This combination will enable the improved management of the operation of a city in an integrated and systematic way, thus promoting the wisdom of urban planning, construction, management, and service.

Acknowledgements

We would like to thank the editor and the reviewers for their invaluable suggestions that improved both the content and the presentation of the paper.

The work was partially supported by the National Natural Science Foundation of China (Grant No. 71603017), National Key R&D Program of China (Grant No. 2017YFC0804706), and the Fundamental Research Funds for the Central Universities (Grant No. 2652017074). Some of the work was also carried out during Dr. Gai's research visit to Professor Salhi at the Centre for Logistics & Heuristic Optimisation (CLHO) in Kent, UK.

References

Carson, F., 2010. Pedestrian walking speed in crosswalk study. Accid. Reconstr. J. 20 (6), 11-15.

Cozzani, V., Gubinelli, G., Antonioni, G., Spadoni, G., Zanelli, S., 2005. The assessment of risk caused by domino effect in quantitative area risk analysis. J. Hazard. Mater. 127 (1-3), 14-30.

Danial, S. N., Smith, J., Khan, F., Veitch, B., 2019. Situation awareness modeling for emergency management on offshore platforms. Hum. Cent. Comput. Inf. Sci. 9(1), 37.

Danial, S. N., Smith, J., Veitch, B., Khan, F.,2019. On the realization of the recognition-primed decision model for artificial agents. Hum. Cent. Comput. Inf. Sci. 9(1), 36.

Deng, Y. F., Jiang, C. S., 2009. Survey on the public evacuation behavior in"4·16"accident at Tianyuan chemical factory of Chongqing. J. Saf. Sci. Technol. 5 (3), 31-36(in Chinese).

Ding, X. Y., Jiang, J. C., Huang, Q., 2007. Simulation analysis on release and dispersion process of liquefied ammonia tank. J. Saf. Sci. Technol. 3 (3),7-11(in Chinese).

Ding, L., Ji, J., Khan, F., 2020. Combining uncertainty reasoning and deterministic modeling for risk analysis of fire-induced domino effects. Saf. Sci. 129, 104802.

Gai, W. M., Deng, Y. F., 2019. Survey-based analysis on the diffusion of evacuation advisory warnings during regional evacuations for accidents that release toxic vapors: a case study. J. Loss Prev. Process Ind. 57, 174-185.

Georgiadou, P. S., Papazoglou, I. A., Kiranoudis, C. T., Markatos, N. C., 2010. Multi-objective evolutionary emergency response optimization for major accidents. J. Hazard. Mater. 178, 792-803.

Georgiadou, P. S., Papazoglou, I. A., Kiranoudis, C. T., Markatos, N. C., 2007. Modeling emergency evacuation for major hazard industrial sites. Reliab. Eng. Syst. Saf. 92, 1388-1402.
Jeong, G. S., Baik, E. S., 2018. Damage Effects Modeling by Chlorine Leaks of Chemical Plants. Fire. Sci. Eng, 32(3), 76-87.
Hong, L., Gao, J., Zhu, W.,2018. Self-evacuation modelling and simulation of passengers in metro stations. Saf. Sci. 110, 127-133.
Hosseinnia, B., Khakzad, N., Reniers, G., 2018. Multi-plant emergency response for tackling major accidents in chemical industrial areas. Saf. Sci. 102, 275-289.
Huang, X.Y., Chen, W., 1999. Aging of the world's population: trends and patterns. Popul Res. 3, 54-59.
Jann, P. R., 1989. Evaluation of temporary safe havens. J. Loss Prev. Process Ind. 2, 33-38.
Hu, J., Sun, H., Gao, G., Wei, J., You, L.,2014. The group evacuation behavior based on fire effect in the complicated three-dimensional space. Math. Prob. Eng. 2014(4), 1-7.
Jia, M., Chen, G., Reniers, G., 2017. Equipment vulnerability assessment (eva) and pre-control of domino effects using a five-level hierarchical framework (flhf). J. Loss Prev. Process Ind. 48, 260-269.
Khakzad, N., 2018. Which fire to extinguish first? a risk-informed approach to emergency response in oil terminals. Risk Anal. 38(7), 1444-1454.
Kim, H., Park, M., Kim, C. W., Shin, D., 2019. Feed-forward neural networks and recurrent neural networks for locating the leak point of chemicals in outdoor plant: a combination of deep-learning and cfd simulation. Comp. Chem. Eng. 125, 476-489. doi: https://doi.org/10.1016/j.compchemeng.2019.03.012.
Lindell, M. K., 2008. Emblem2: an empirically based large scale evacuation time estimate model. Transport. Res. A-Pol. 42(1), 140-154.
Mardle, S., Miettinen, K. M., 2000. Nonlinear multi objective optimization. J. Oper. Res. Soc. 51(2), 246.
Menz, H. B., Latt, M. D., Tiedemann, A., San Kwan, M. M., Lord, S. R. 2004. Reliability of the GAITRite® walkway system for the quantification of temporo-spatial parameters of gait in young and older people. Gait. Posture. 20 (1), 20-25.
Musharraf, M., Smith, J., Khan, F., Veitch, B., Mackinnon, S.,2016. Assessing offshore emergency evacuation behavior in a virtual environment using a bayesian network approach. Reliab. Eng. Syst. Saf. 152(Aug.), 28-37.
Norafneeza, N., Faisal, K., Brian, V., Scott, M. K.,2018. Dynamic risk assessment of escape and evacuation on offshore installations in a harsh environment. Appl. Ocean Res. 79, 1-6.
Norazahar, N., Khan, F., Veitch, B., Mackinnon, S.,2015. Assessing Evacuation Operation Performance in Harsh Environments. ASME 2015 34th International Conference on Ocean, Offshore and Arctic Engineering.1,1-6. doi: https://doi.org/10.1115/omae2015-41428.
Norazahar, N., Faisal, K., Brian, V., Scott, M.K., 2014. Human and organizational factors assessment of the evacuation operation of BP Deepwater Horizon accident. Saf. Sci. 70, 41-49
OGP, 2010. Risk Assessment Data Directory: Vulnerability of humans, International Association of Oil and Gas Procedures, Report 434–14.1.

Reniers, G., Soudan, K., 2010. A game-theoretical approach for reciprocal security-related prevention investment decisions. Reliab. Eng. Syst. Saf. 95, 1-9.
Sharma, S., 2009 Simulation and modeling of group behavior during emergency evacuation. In 2009 IEEE Symposium on Intelligent Agents. 122-127. IEEE.
Shi, C., Zhong, M., Nong, X., He, L., Shi, J., Feng, G., 2012. Modeling and safety strategy of passenger evacuation in a metro station in china. Saf. Sci. 50(5), 1319-1332.
Shimbel, A., 1953. Structural parameters of communication networks. B. Math. Biophys. 15(4), 501-507.
Sorensen, J. H., Shumpert, B. L., Vogt, B. M., 2004. Planning for protective action decision making: evacuate or shelter-in-place. J. Hazard. Mater. 109, 1-11.
Smith, J., Musharraf, M., Veitch, B., 2017. Data informed cognitive modelling of offshore emergency egress behaviour. Proceedings of the 15th International Conference on Cognitive Modeling. 146-151. Coventry, United Kingdom: University of Warwick.
Stepanov, A., Smith, M. G., 2009. Multi-objective evacuation routing in transportation networks. Eur. J. Oper. Res. 198, 435-446.
Ujihara, A. M., 1989. Responding to chemical accidents by sheltering in place. Resources, 94.
Vermuyten, H., Beliën, J., De Boeck, L., Reniers, G., Wauters, T., 2016. A review of optimisation models for pedestrian evacuation and design problems. Saf. Sci. 87, 167-178.
Xiao, G. Q., Wen, L. M., Chen, B. Z., Wang, H., 2001.Shortest Evacuation Path on Toxic Leakage. J. Northeast. Univ. 22, 674-677.
Yadav, K., Biswas, R., 2010. An intelligent search path. Int. J. Intell. Syst. 25(9), 970-980.
Yi, W., ÖZdamar, L., 2007. A dynamic logistics coordination model for evacuation and support in disaster response activities. Eur. J. Oper. Res. 179(3), 1177-1193.
Yoo, B., Choi, S. D., 2019.Emergency Evacuation Plan for Hazardous Chemicals Leakage Accidents Using GIS-based Risk Analysis Techniques in South Korea. Int. J. Env. Res. Pub. He. 16(11): 1948
Yuan, Y., Wang, D., 2009. Path selection model and algorithm for emergency logistics management. Comput. Ind. Eng. 56, 1081-1094.
Zhang, J. H., Liu, H. Y., Zhu, R., Liu, Y., 2017. Emergency evacuation of hazardous chemical accidents based on diffusion simulation. Complexity, 2017, 1-16.
Zhang, X., Zhang, Z., Zhang, Y., Wei, D., Deng, Y., 2013. Path selection for emergency logistics management: A bio-inspired algorithm. Saf. Sci. 54, 87-91.
Zhou, Y., Liu, M., 2012. Risk assessment of major hazards and its application in urban planning: a case study. Risk Anal. 32(3), 566-577.

Appendix 1: The optimal route planning results for each node based on Model I and Model II

Optimization model	Model I			Model II		
Optimization objectives	Mitigation of health consequences			Minimizing transfer time		
	route	**dose**	**transfer time (min)**	**route**	**dose**	**transfer time (min)**
Optimization goals	1→11→16→ 18→ 13→ 9→ 14→ 15→ 20	8.88E+10	33.94	1→ 11→ 16→ 17→ 18→ 19→ 20	9.29E+10	13.65
	2→ 7→ 8	4.41E-17	3.54	2→ 7→ 8	4.41E-17	3.54
	3→ 4→ 8	4.09E-17	3.76	3→ 8	4.75E-17	1.83
	4→ 8	3.83E-17	1.48	4→ 8	3.83E-17	1.48
	5→ 10→ 15→ 20	1.52E+08	11.23	5→ 10→ 15→ 20	1.52E+08	11.23
	6→ 12→ 8	1.44E+10	2.31	6→ 12→ 8	1.44E+10	2.31
	7→8	3.77E-17	1.45	7→8	3.77E-17	1.45
	8	0	0	8	0	0
	9→ 14→ 15→ 20	1.47E+08	8.43	9→ 14→ 15→ 20	1.47E+08	8.43
	10→ 15→ 20	1.52E+08	8.07	10→ 15→ 20	1.52E+08	8.07
	11→ 16→ 18→ 20	6.52E+08	13.49	11→ 16→ 17→ 18→ 19→ 20	4.34E+09	11.07
	12→8	224	2.04	12→8	224	2.04
	13→ 8	127	3.65	13→ 8	127	3.65
	14→ 15→ 20	1.47E+08	7.20	14→ 15→ 20	1.47E+08	7.20
	15→ 20	1.42E+08	5.76	15→ 20	1.42E+08	5.76
	16→ 18→ 20	5.68E+08	9.81	16→ 17→ 18→ 20	3.82E+09	8.13
	17→ 12→ 8	7.71E+08	3.47	17→ 12→ 8	7.71E+08	3.47
	18→ 20	2.37E+08	2.95	18→ 20	2.37E+08	2.95
	19→ 20	2.02E+08	2.46	19→ 20	2.02E+08	2.46
	20	0	0	20	0	0

Appendix 2: Multi-objective optimization results of emergency route selected based on Model III

Route	dose	transfer time (min)	Route	dose	transfer time (min)
1→11→16→18→19→20	8.88E+10	15.71	11→16→18→20	6.52E+08	13.49
2→7→8→13→19→20	2.84E+08	12.12	12→8→4→9→14→15→20	1.47E+08	15.51
3→4→9→14→15→20	1.47E+08	13.97	13→9→14→15→20	1.47E+08	10.85
4→9→14→15→20	1.47E+08	11.65	14→15→20	1.47E+08	7.20
5→10→15→20	1.52E+08	11.23	15→20	1.42E+08	5.76
6→12→8→ 13→19→20	1.47E+10	13.16	16→18→20	5.68E+08	9.81
7→8→4→9→14→15→20	1.47E+08	14.86	17→13→9→14→15→20	1.69E+09	14.00
8→4→9→14→15→20	1.47E+08	13.23	18→ 20	2.37E+08	2.95
9→14→15→20	1.47E+08	8.43	19→ 20	2.02E+08	2.46
10→15→20	1.52E+08	8.07	20	0	0